Variation of Gravure Coating Thickness During Early Stages of Doctor Blade Wear

R. Hanumanthu
Manufacturing Research & Engineering, Eastman Kodak Co., Rochester, NY 14652

With all operating parameters fixed, the mean coated thickness in gravure coating should ideally be a constant fraction of the volume factor of the engraving, and, hence, invariant over coated distance. Experimental data presented, however, reveal an unexpected variation of gravure coating thickness over the first few thousand meters of coated web. The observed variation is attributed to wear of the blade tip. The lubrication approximation is invoked to model a series of steady-state flows between blade tips of various profiles and a smooth surface at a fixed gap away from them. The blade tip profiles are chosen to simulate those of a continously wearing blade tip. The resulting four-parameter model is used to ''fit'' experimental data of gravure coating thickness variation. Then, the model is used to predict the effects of various operating parameters, including coating liquid properties, blade thickness, blade setup, and web speed, on this phenomenon.

Introduction

In the gravure coating/printing process (see Figure 1), coating liquid is first applied to the surface of an engraved cylinder, most commonly by rotating the latter through a pool of liquid, but other feed methods have also been reported (Coyle and Fitzgerald, 1996; Lobo et al., 1997). The engraving, usually an array of grooves or ''cells,'' may be continuous over the surface of the cylinder or in the form of discrete patches or other patterns. Subsequent to the feed step, a doctor blade removes liquid in excess of that needed to fill the cells. The liquid retained by the cells is then applied to the surface of a moving web by impressing the latter between the engraved cylinder and a rubber-covered backing roll.

The mean thickness of the coating thus transferred is usually a known fraction of the volume of engraved cells per unit surface area of the gravure cylinder, that is, the *volume factor* of the engraving. This ''fraction transferred'' depends on engraving design (cell dimensions, number of cells per unit surface area of the cylinder, and so on), pressure on the backing roll and softness of its rubber cover, liquid properties including rheology and surface tension, and gravure cylinder/backing roll speeds and directions of rotation (Hanumanthu, 1996).

In addition to the parameters listed above, gravure coating thickness depends critically on the doctoring process, or, more specifically, on the volume of liquid in the cells, downstream of the doctor blade. This volume may be equal to, greater than, or less than that needed to exactly fill the cells; and it is determined by the complex elastohydrodynamic interactions between cylinder engraving, liquid flow, blade flexibility, and blade load (Kistler 1988). However, at *fixed* doctoring conditions, the metered volume is again chiefly a function of the volume factor (Kistler, 1988).

Therefore, the key to successful gravure coating is the control of mean coating thickness via the volume factor alone-and the invariability of the relationship between the two-once all other parameters are fixed.

However, recent experiments conducted on a pilot gravure coating machine at Eastman Kodak Company revealed a variation in coating thickness, even when all operating parameters were fixed (see Figure 2). In Figure 2, the abscissa has been reported as a coated distance, namely, the product of coating speed and time. The ordinate has been represented as a ratio of mean coated thickness to volume factor of the engraving. Thus, the coating thickness was initially about 58% of the volume factor and it asymptotically reduced to 50% of the volume factor over the first few thousand meters of coated web. The thickness then stayed steady

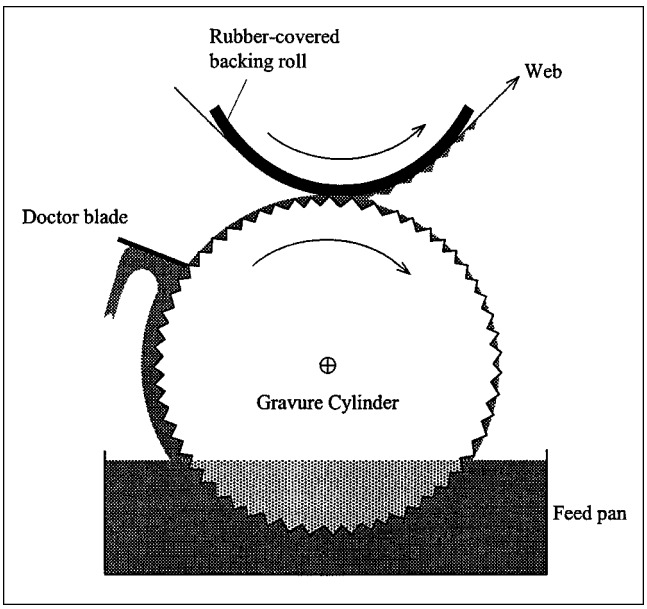

Figure 1. Gravure coating process.

Coating liquid is applied to the surface of an engraved cylinder; a doctor blade removes excess liquid; a fraction of the liquid remaining in the cells is transferred to the moving web.

at the 50% value for the next several thousand meters of coated web (data not shown in Figure 2). The Reynolds' number of the flow (product of volume factor, liquid density, coating speed, and inverse of liquid viscosity) was 0.31, and the capillary number (product of liquid viscosity, coating speed, and inverse of liquid surface tension) was 1.2. The gravure cylinder and backing roll were rotated at equal surface speeds in angular directions opposing each other, that is, in the ''forward'' roll coating mode. The engraved cells were ''pyramidal,'' with a triangular cross-section in the axial direction of the cylinder, and a sinusoidal cross-section in the azimuthal direction (Walters and Lobo, 1995). Further, the cells

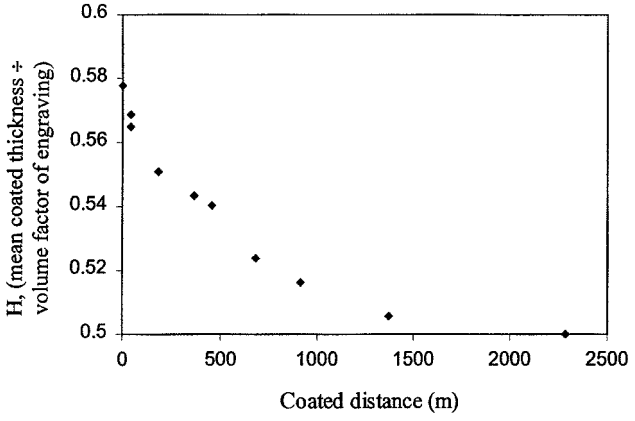

Figure 2. Experimental measurements of mean coating thickness in gravure coating.

Thickness was initially about 58% of the volume factor of the engraving. As coating proceeded, thickness reduced to an asymptotic value of 50%.

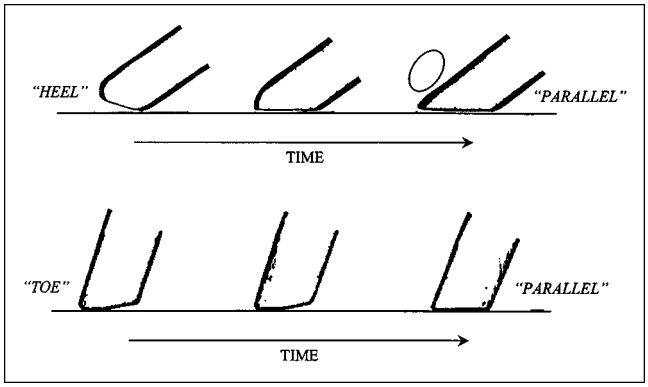

Figure 3. Magnified, cross-sectional images of the tips of doctor blades taken off a gravure coating machine at various points of time after the start of coating.

Profiles clearly show the wear of the blade tip from either ''heel'' or ''toe'' configurations down to a ''parallel'' configuration.

were connected in the azimuthal direction by channels. These channels promote leveling of the transferred coating, yielding, ultimately, a smooth and uniform coated layer.

In the work presented herein, the variation of mean coating thickness observed in the experimental measurements is attributed to *wear* of the blade tip. That the tip of the blade does indeed wear during gravure coating operation is evidenced by the micrographs in Figure 3. In fact, materials of construction of doctor blades are chosen to be softer than those of the cylinder, so that the blade wears in preference to the cylinder surface (Rutherford, 1991). Figure 3 presents magnified, cross-sectional images of the tips of doctor blades taken off a gravure coating machine at various points of time after the start of coating. The two initial configurations shown-''toe'' and ''heel''-depend on blade setup conditions.

Effects of Blade Setup and Blade Tip Wear

Doctor blades are typically purchased with a prescribed ''bevel'' angle, θ_b (Max Daetwyler Corp., 1994). They are then mounted at a specified ''tangent'' angle θ_t° relative to the cylinder surface. When a load is applied on the blade during coating operation, the blade flexes, and the *operating* tangent angle θ_t is less than the setup tangent angle θ_t° (see Figure 4).

Then, depending on the relation between θ_t and θ_b, that is, whether θ_t is equal to, greater than, or less than θ_b, the tip of the blade is initially either ''parallel'' to the cylinder surface, or the blade is riding on its ''toe,'' or on its ''heel'' (Figure 5). Subsequently, as the tip of the blade wears, both toe- and heel-gap configurations wear down to the parallel-gap configuration (see Figure 6, and micrographs in Figure 3).

The mean thickness of liquid on the gravure cylinder downstream of the blade depends on the rate of flow of liquid between the tip of the blade and the moving cylinder surface (Figure 7). The nominal blade tip thickness t, is usually 3–4 orders of magnitude less than the radius of the

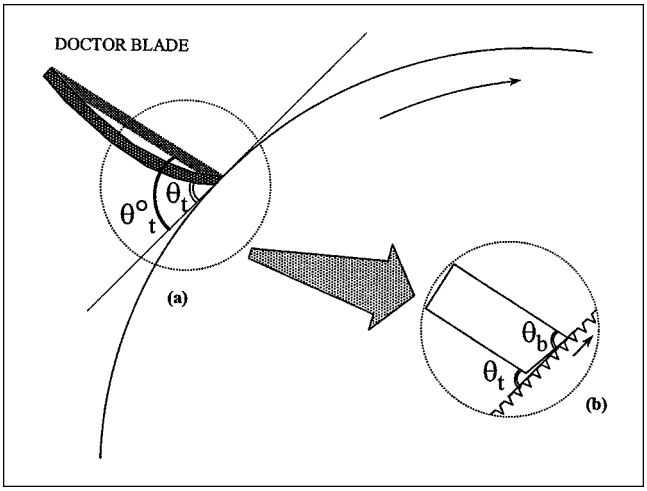

Figure 4. (a) Doctor blades set up to make the blade a prescribed "tangent" angle, θ_t°, with the tangent to the roll surface at the point of contact between the two.

When the blade is loaded, it flexes, and the operating tangent angle θ_t is less than θ_t°. (b) magnified view of the tip of the blade with the pre-sharpened "bevel angle" of the blade θ_b.

gravure cylinder. Hence, in Figure 7, and for the remainder of this report, the effects of cylinder radius are neglected and cylinder surface is treated as essentially flat relative to the tip of the blade.

When the maximum height H of the gap between the tip of the blade and the moving cylinder is much smaller than the length of the flow channel L, the lubrication approximation (Cameron, 1976) of nearly-rectilinear flow applies. Then, the total flow rate per unit width between the blade and the cylinder can be expressed as the sum of a pressure-driven (that is, Poiseuille) contribution and a drag (or Couette) contribution

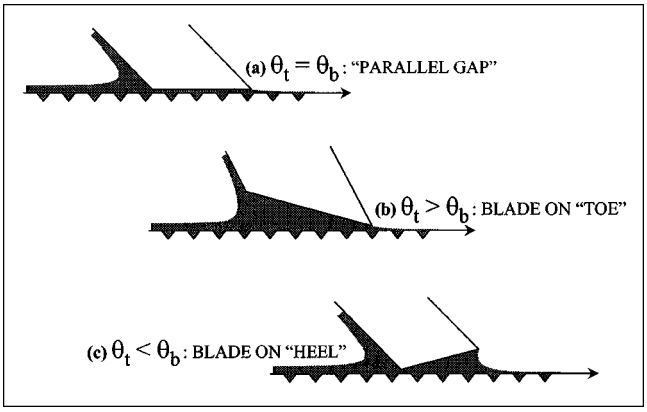

Figure 5. Depending on the relationship between the operating tangent angle θ_t and the blade bevel angle θ_b the blade is riding on its "toe" ($\theta_t > \theta_b$), or "heel" ($\theta_t < \theta_b$), or the gap between the tip of the blade and the moving cylinder is parallel ($\theta_t = \theta_b$).

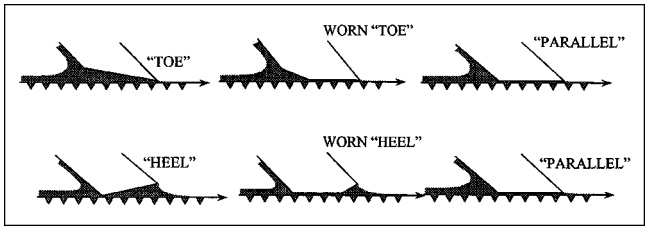

Figure 6. As the tip of the blade wears, both "toe" and "heel" configurations of Figures 5b and 5c approach the parallel-gap configuration of Figure 5a.

$$q_x = \frac{-h_p^3}{12\mu}\frac{\Delta P}{L} + \frac{h_d}{2}U \tag{1}$$

where L is the length of the flow channel measured in the x-direction, ΔP is the pressure drop across the channel, μ is the viscosity of liquid, and U is surface speed of the gravure cylinder. h_p and h_d are, respectively, the effective average heights of the gap for pressure-driven and drag flows. From Eq. 1, the mean thickness h_c on the cylinder surface downstream of the blade is simply

$$h_c = \frac{q_x}{U} = \frac{-h_p^3}{12\mu U}\frac{\Delta P}{L} + \frac{h_d}{2}. \tag{2}$$

The lubrication approximation becomes less accurate as the gap length L shortens until it is comparable to either height h_p or h_d.

The effective average gaps h_p and h_d for pressure-driven and drag flows, respectively, are defined for a nonuniform gap distribution $h(x)$ as (Higgins and Scriven 1980)

$$h_p^3 \equiv \frac{L}{\int_0^L [h(x)]^{-3}\,dx} \tag{3}$$

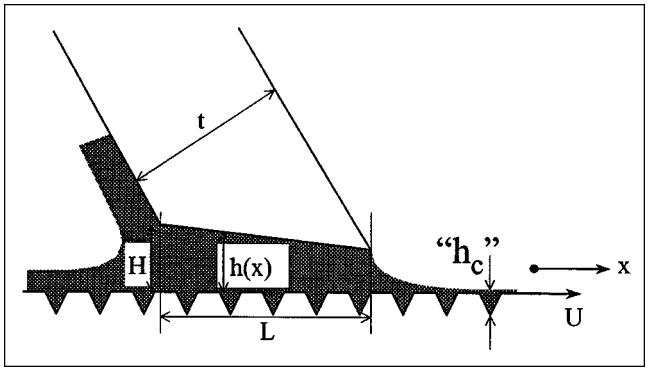

Figure 7. If $H \ll L$, the flow between the tip of the blade and the moving roll surface is nearly rectilinear, and lubrication theory applies to this flow.

and

$$h_d \equiv \frac{\int_0^L [h(x)]^{-2}\,dx}{\int_0^L [h(x)]^{-3}\,dx}. \tag{4}$$

It is evident from Eq. 2 that, all else remaining the same, the mean doctored thickness h_c depends critically on the effective pressure-driven and drag heights h_p and h_d. And, clearly, in both the ''toe'' and ''heel'' cases of Figures 5b and 5c, the effective height of the gap between the blade tip and the gravure cylinder surface is larger than that in the ''parallel gap'' case (Figure 5a).

Further, as the tip of the blade wears, both toe- and heel-gap configurations wear down to the parallel-gap configuration (Figure 6). Consequently, the effective Couette and Poiseuille heights of the gap between blade tip and cylinder decrease with coated distance, until the parallel-gap configuration is attained. Correspondingly, coating thickness, as seen in Figure 2, reduces asymptotically until it attains the value for the parallel-gap case.

Model of Flow Coupled with Wear

The flow between the engraved cylinder and blade is not only three-dimensional, but also time-dependent. In addition, since the blade wears, the flow between the blade and at least the unengraved areas of the cylinder is in the regime of boundary lubrication. All these factors render modeling of the flow an intimidating task. However, the primary goal of this work is not to model the flow between the engraved cylinder and the tip of the blade. Rather, it is to determine if the excess flow under a blade that is riding on its toe or heel-compared to when its tip is parallel to the substrate-and the rate of change of that flow rate as the profile of the blade tip changes, (for example, due to wear), are sufficient to explain the variation of thickness observed in the data of Figure 2.

To that end, the model focuses on the steady-state flow between a blade and a moving, *smooth* surface at a fixed gap from it. The calculation is repeated for several such flows, each with a different profile of the blade tip. The changing blade tip profile is modeled after a continuously wearing blade.

Additionally, it is assumed that the change in length of the blade as its tip wears from a toe- or heel-gap configuration to a parallel-gap configuration is so small that the operating tangent angle θ_t stays constant during the process-and so does the applied load on the blade.

Figure 8 then represents various blade tip profiles, and a moving, smooth substrate at a fixed gap h_m away from them. In Figure 8, y represents the vertical distance worn, perpendicular to the direction of movement of the substrate. Therefore, when $y = 0$, the blade tip is new (unworn), and the length of the flow channel is L_0. When $y = y_m$, the tip of the blade attains the parallel-gap configuration, and the length of the flow channel is L_f. When $0 < y < y_m$, the tip of the blade is partially worn. Then, L is the length of the flow channel. Further, $L = L_1 + L_2$, where L_1 is the length of the flow channel corresponding to the unworn portion of the blade, and L_2 is the worn length of the blade tip (see Figure 8).

The following relationships are evident

$$L_0 = \frac{t\cos|\theta_t - \theta_b|}{\sin\theta_b}; \tag{5}$$

$$L_f = \frac{t}{\sin\theta_t}; \text{ and} \tag{6}$$

$$y_m = \frac{t\sin|\theta_t - \theta_b|}{\sin\theta_b}; \tag{7}$$

where t is the thickness of the blade tip, θ_t is the operating tangent angle, and θ_b is the bevel angle of the blade.

The lubrication equation of flow, applied to any of the configurations in Figure 8, is

$$h_c = \frac{-h_p^3}{12\mu U}\frac{\Delta P}{L} + \frac{h_d}{2}. \tag{8}$$

The effective average gaps h_p and h_d for pressure-driven and drag flows, respectively, have been defined for a nonuniform gap distribution $h(x)$ in Eqs. 3 and 4. As shown in Figure 8, for a partially worn blade, $h(x)$ is linear between $x = 0$ and $x = L_1$, and is uniformly equal to h_m between $x = L_1$ and $x = L_1 + L_2 = L$.

The various lengths are expressed in units of the minimum gap h_m, that is $H_c = h_c/h_m$; $H_p = h_p/h_m$; $H_d = h_d/h_m$; $Y = Y/h_m$; and $L^* = L/h_m$. Pressure is expressed in units of $\mu U/h_m$, that is, $\pi = P/(\mu U/h_m)$.

Then, in terms of dimensionless quantities, Eq. 8 is rewritten as

$$H_c = \frac{-\Delta\pi}{12L^*}H_p^3 + \frac{H_d}{2}. \tag{9}$$

The details of the evaluation of the integrals in Eqs. 3 and 4 for the partially-worn blade tip profile are omitted here, but the result, after substitution back into Eq. 9, is

$$H_c = \frac{1}{2}\frac{\left[\dfrac{-\Delta\pi}{6} + \dfrac{L_1^*}{C} + L_2^*\right]}{\left[\dfrac{L_1^*(1+C)}{2C^2} + L_2^*\right]}. \tag{10}$$

Here

$$L_1^* = (1 - Y/Y_m)\,L_o^*; \tag{11}$$

$$L_2^* = (Y/Y_m)\,L_f^* \tag{12}$$

and

$$C = Y_m(1 - Y/Y_m) + 1. \tag{13}$$

In the equations above, Y_m, L_o^*, and L_f^* are now in units of

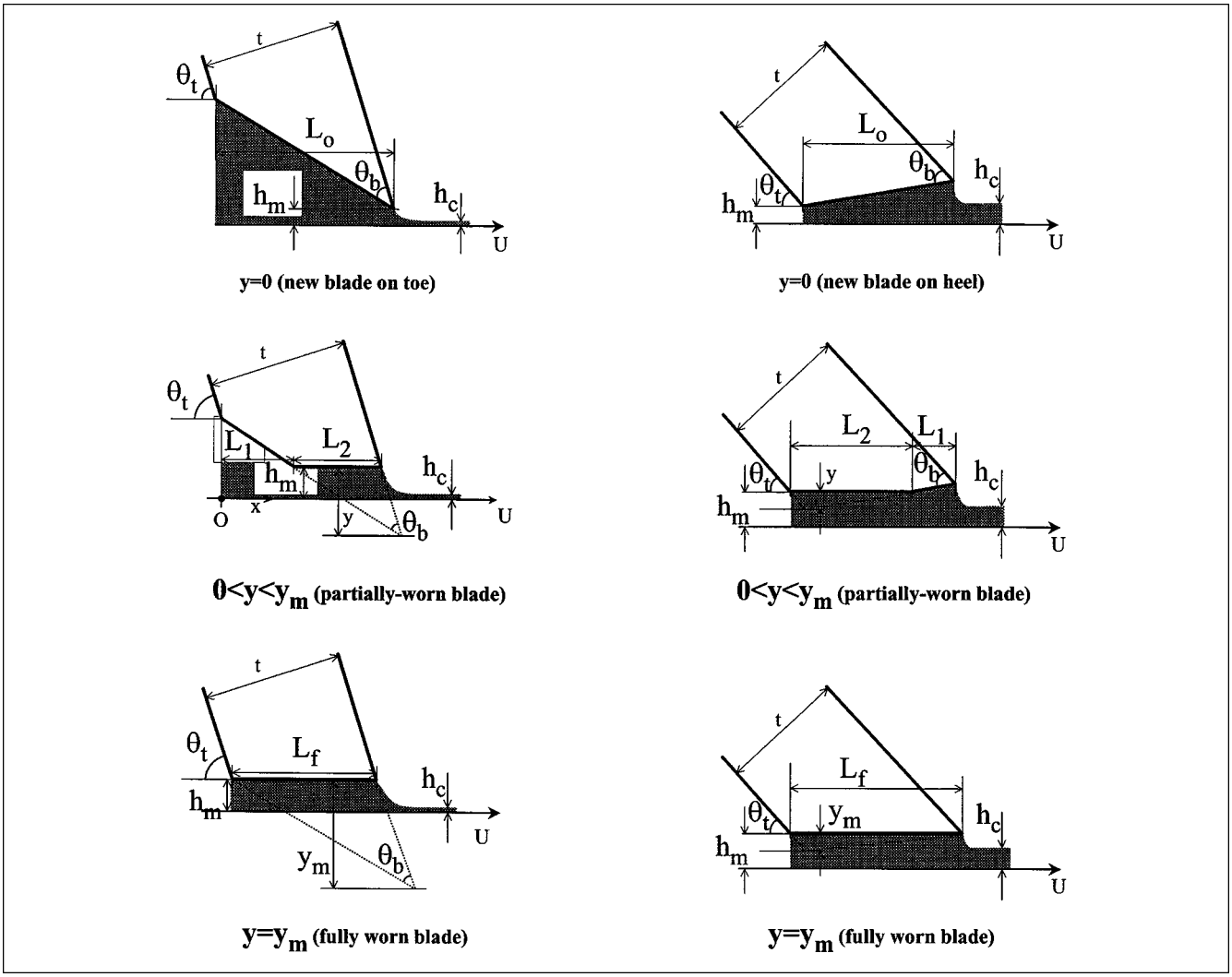

Figure 8. Steady-state-flow between a moving, smooth surface and blade tips whose profiles are changing.

Dotted-line triangles represent portions of the blade tip that might be removed by wear.

h_m, that is

$$L_o^* = \frac{T\cos|\theta_t - \theta_b|}{\sin\theta_b} \tag{14}$$

$$L_f^* = \frac{T}{\sin\theta_t} \tag{15}$$

and

$$Y_m = \frac{T\sin|\theta_t - \theta_b|}{\sin\theta_b}; \tag{16}$$

where T is the thickness of the tip of the blade in units of the minimum gap h_m.

Finally, because the ultimate goal of the model is to predict mean coating thickness variation as the blade wears, *relative* to the thickness when it is fully worn, the calculated mean thickness H_c(Eq. 10) is further scaled by the coating thickness when the blade tip is fully worn, that is, when $Y/Y_m = 1$. This scaled thickness is

$$H_c^* = \frac{\left[\dfrac{-\Delta\pi}{6} + \dfrac{L_1^*}{C} + L_2^*\right] \Big/ \left[\dfrac{L_1^*(1+C)}{2C^2} + L_2^*\right]}{\left[\dfrac{-\Delta\pi}{6L_f^*} + 1\right]}. \tag{17}$$

Wear equation

To relate the vertical distance worn y to the coated distance represented by the abscissa of Figure 2, the law of adhesive wear (Rabinowicz, 1995) is invoked. This law states that

$$\text{Volume worn} \propto (\text{Loading force} \times \text{Sliding distance}) \div (\text{Hardness of surface being worn}). \tag{18}$$

The proportionality constant in the above equation includes the coefficient of wear. In this work, the proportionality constant, the loading force per unit width of the blade, and blade hardness are combined into a single, phenomenological constant Ψ. This constant has units of length, but here it is expressed in units of h_m. Then, on a per-unit-width basis, Eq. 18 becomes

$$\text{Area worn} \equiv 0.5\ L_2^* Y = \Psi X_s, \tag{19}$$

where X_s is the dimensionless sliding distance, and it is equivalent to the ''coated distance'' referred to in Figure 2.

Now, when $Y = Y_m$, $L_2^* = L_f^*$ (from Eq. 12); therefore, from Eq. 19

$$0.5\ L_f^* Y_m = \Psi X_{s,m}. \tag{20}$$

$X_{s,m}$ now represents the coated distance (in units of h_m) when the tip of the blade wears down to the parallel-gap configuration. Per assumptions made earlier on, the constant Ψ, does not change as the tip of the blade wears. Combining Eqs. 19, 20, and 12, we have

$$\left(\frac{Y}{Y_m}\right) = \sqrt{\frac{X_s}{X_{s,m}}}\ . \tag{21}$$

Thus, for a given blade tip thickness T and setup conditions θ_b and θ_t, mean coating thickness is estimated from Eqs. 11—17, and Eq. 21, with $0 \le X_s/X_{s,m} \le 1$.

Results and Discussion

Equations 11 through 17 represent a four-parameter model, with the parameters being $\Delta\pi$, T, θ_t and θ_b. In the experiments of Figure 2, θ_t and θ_b were determined by measurements off micrographs of the blade tips, similar to those shown in Figure 3. The bevel angle θ_b measured off a new blade was 55°c, and the tangent angle θ_t measured off a worn blade was 60°. Unfortunately, the pressure drop across the flow channel $\Delta\pi$ is unknown for the experiments. Moreover, the blade tip thickness t was measured, but since the minimum gap h_m (Figure 8) in the lubrication model is arbitrary, the experimental equivalent of the dimensionless thickness T could not be estimated. Therefore, in the attempt to fit the experimental data of Figure 2 to predictions from the model, arbitrary choices of $\Delta\pi$ and T were made.

To simplify the analysis that follows, the pressure drop across the channel was initially neglected, that is, $\Delta\pi = 0$. This approximation is accurate as long as upstream and downstream pressures in the liquid are close to ambient, and inertial and surface tension forces are small. The value of T was ''dialed-in'' until the best fit was obtained.

The data of Figure 2 was further manipulated to make the axes of experimental and theoretical plots compatible: first, the ordinate of the plot in Figure 2 was scaled by 50%-the asymptotic value of the measured mean thickness as a fraction of volume factor of engraving. Secondly, the abscissa of Figure 2 was scaled by 2,280 m, which is the length of coated web ($\equiv x_{s,m}$) when the measured thickness has attained its asymptotic value.

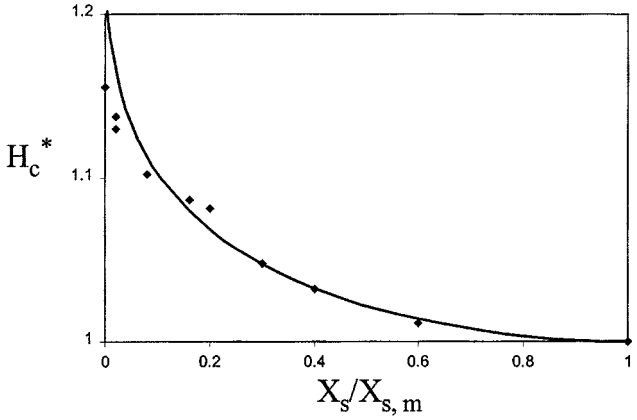

Figure 9. Predictions of the lubrication model (——) are superimposed over the experimental data of Figure 2 (♦).

Agreement between the two is within 3%, when $\Delta\pi = 0$, and $T = 6$. In both theory and experiment, $\theta_t = 60°$, $\theta_b = 55°$.

Thus, Figure 9 superimposes the theoretical predictions of the lubrication model and the experimental data of Figure 2. With $\Delta\pi = 0$ and $T = 6$, the theoretical curve fits experimental data well-the agreement between the two is within 3% except at very short coating distances. The discrepancy there can be attributed to error in the experimental measurements, as coating does not begin the instant the blade starts wearing. Typically, the blade is first lowered against the gravure cylinder, while the cylinder is rotating at a slow, ''idle'' speed. Then, the cylinder is sped up. Once the cylinder has reached the desired operating speed, the web and backing roll are lowered. During this time, the blade has been wearing, and as the slope of the predicted curve in Figure 9 suggests, the very initial period of wear is accompanied by a rapid drop in the mean coating thickness. As wear proceeds, the fit between predictions of the lubrication model and experimental data of gravure coating thickness further improves.

The model is hence used as a predictive tool to study the effects of operating parameters on the phenomenon of gravure coating variation during early stages of coating, or, per the hypothesis presented here, the early stages of doctor blade wear.

Figures 10 and 11 show the effects of bevel angle and tangent angle at $\Delta\pi = 0$ and $T = 6$. Clearly, the greater the difference between tangent and bevel angles, that is, the higher the blade rides on its toe or heel, the larger is the departure of the mean coating thickness from its asymptotic value. Moreover, both Figures 10 and 11 suggest that a blade riding on its heel shows a faster reduction in thickness with wear than a blade on its toe. This is explained as follows: when $\Delta\pi = 0$, Eq. 17 reduces to

$$H_c^*(\Delta\pi = 0) = \frac{\left[\dfrac{L_1^*}{C} + L_2^*\right]}{\left[\dfrac{L_1^*(1+C)}{2C^2} + L_2^*\right]}. \tag{22}$$

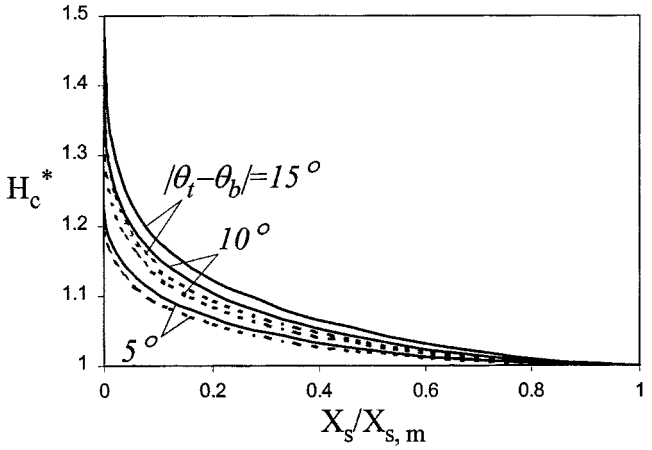

Figure 10. Effect of bevel angle θ_b at a fixed tangent angle $\theta_t = 60°$.

Solid lines represent the toe-configuration ($\theta_t > \theta_b$), whereas dashed lines are for the heel-configuration ($\theta_t < \theta_b$). Blade tip thickness, $T = 6$, $\Delta\pi = 0$.

Both numerator and denominator of the ratio on the right-hand side of the above equation grow as Y/Y_m rises from 0 to 1. However, since the ratio itself decreases (see Figure 9), the denominator must grow faster than the numerator. Figure 12a shows the rise in the denominator when θ_t is constant, and Figure 12b is the same at constant θ_b. In both cases, the denominator of the righthand side of Eq. 22 grows faster when the blade is on its heel than when it is on its toe. Consequently, a blade riding on its heel shows a faster decay in mean thickness to the asymptotic value.

Finally, the theoretical model is used to predict the effects of blade tip thickness T and pressure drop $\Delta\pi$ by varying them one at a time.

Thus, Figure 13 shows the effect of blade tip thickness at $\Delta\pi = 0$. The thicker the blade tip, the larger the excess flow.

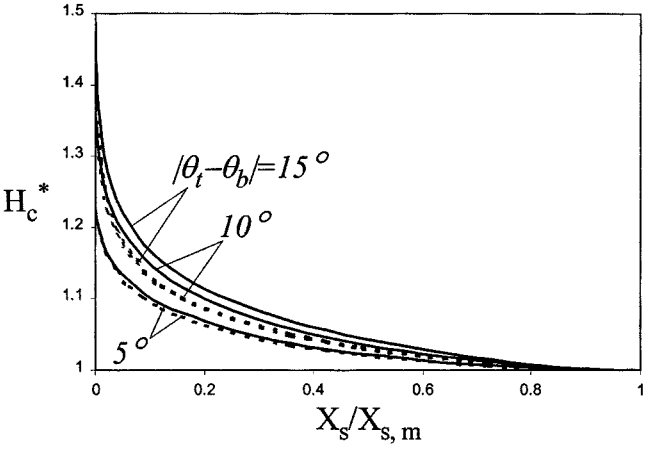

Figure 11. Effect of tangent angle θ_t at a fixed bevel angle $\theta_b = 55°$.

Solid lines represent the toe-configuration ($\theta_t > \theta_b$), whereas dashed lines are for the heel-configuration ($\theta_t < \theta_b$). Blade tip thickness $T = 6$, $\Delta\pi = 0$.

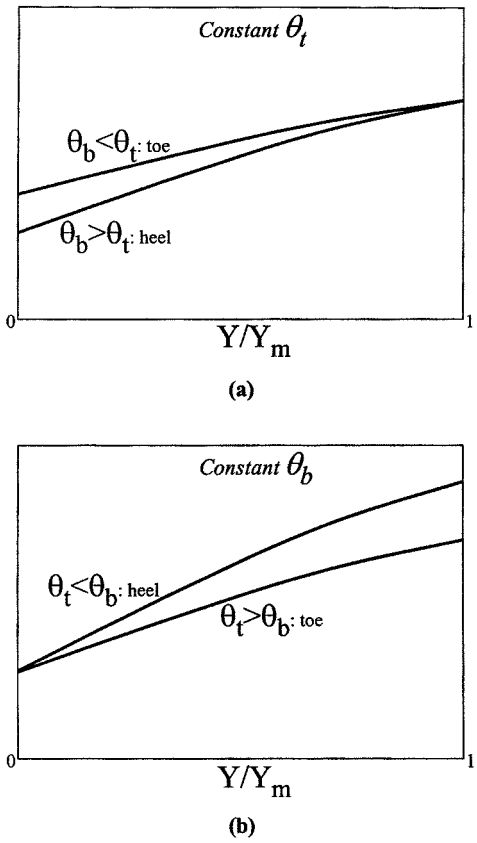

Figure 12. Depictions of the growth of the denominator on the righthand side of Eq. 22.

The effect of pressure drop is the most interesting. As Eq. 10 suggests, the sign of $\Delta\pi$ can play a key role in the magnitude of thickness variation. Physically, the mean coated thickness (see Eq. 10) cannot be negative. This sets an upper, positive bound on the pressure

$$\Delta\pi < \frac{L_1^*}{C} + L_2^*. \tag{23}$$

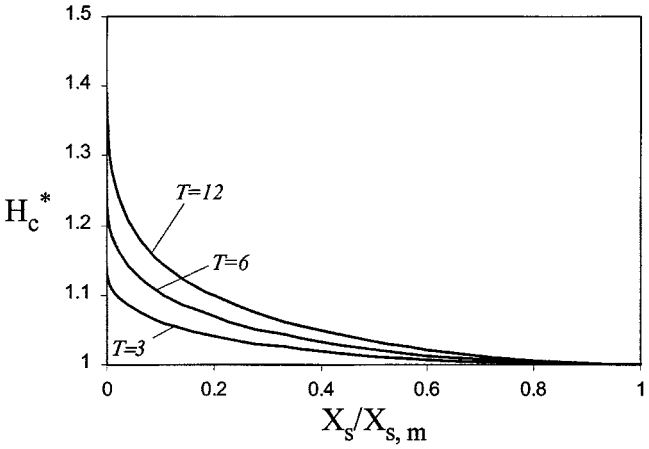

Figure 13. Effect of blade tip thickness *T*.

$\theta_t = 60°$, $\theta_b = 55°$, $\Delta\pi = 0$.

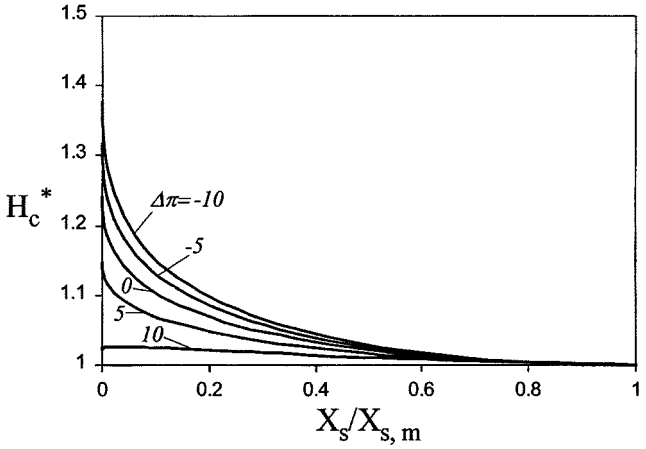

Figure 14. Effect of pressure drop $\Delta\pi$.

$\theta_t = 60°$, $\theta_b = 55°$, $T = 6$.

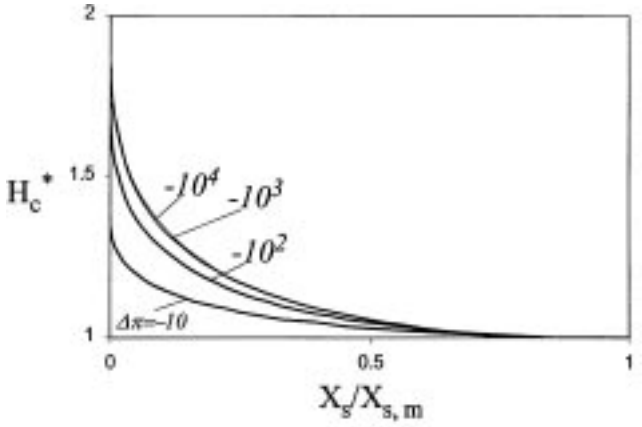

Figure 15. Effect of large, negative pressure drops.

$\theta_t = 60°$, $\theta_b = 55°$, $T = 6$.

However, there is no lower bound. In high-speed blade coating, the flow on the upstream side of the blade is dominated by inertial effects, and pressure there is usually superambient. The pressure in the liquid on the downstream side of the blade is dominated by capillary effects, and it is usually subambient. Then, the pressure drop, defined as the difference between downstream and upstream pressures, is almost always negative. However, if those pressures could be influenced such that their difference became positive, then Figure 14 suggests that the deviation of mean coating thickness from the asymptotic value would be minimized. However, this hypothesis hasn't been verified experimentally.

A second prediction of the proposed model is that as the flow becomes completely dominated by inertia, that is, $\Delta\pi \rightarrow \infty$, the mean thickness becomes independent of the pressure drop

$$H_c^*(\Delta\pi \rightarrow \infty) = \frac{\left[L_f^*\right]}{\left[\frac{L_1^*(1+C)}{2C^2} + L_2^*\right]}. \qquad (24)$$

This effect is seen in Figure 15. Of course, the model assumes that the blade doesn't lift under the influence of these high inertial forces.

In summary, a lubrication model was used to model the steady, nearly rectilinear flow between a blade tip and a smooth surface moving at a fixed gap away from it. The calculation was repeated with varying blade tip profiles. These profiles were chosen to simulate the continuously changing profile of a blade tip as it wears. The four-parameter model thus developed was used to "fit" experimental data of gravure coating thickness during early stages of doctor blade wear. From that time, the model was used to predict the effects of blade setup and other operating parameters on this phenomenon.

To incorporate the effects of wear, the simple law of adhesive wear was invoked. The consequences of using other wear laws was not investigated.

Acknowledgments

The author wishes to thank Dr. L. Flosenzier of Coating Technologies Division, Eastman Kodak Co., for experimental support and key discussions.

Literature Cited

Cameron, A., *Basic Lubrication Theory*, Wiley, New York (1976).
Coyle, D. J., and B. A. Fitzgerald, "Gravure Coating Feeder Apparatus," U.S. Patent No. 5,531,161 (1996).
Hanumanthu, R., "Patterned Roll Coating," PhD Thesis, Univ. of Minnesota, Minneapolis, (available from University Microfilms International, Ann Arbor, MI) (1996).
Higgins, B. G., and L. E. Scriven, "Capillary Pressure and Viscous Pressure Drop Set Bounds on Coating Bead Operability," *Chem. Eng. Sci.*, **35**, 673 (1980).
Kistler, S. F., "Flexible-Blade Doctoring in Gravure Coating," Paper 3b, AIChE Meeting, New Orleans, LA (1988).
Lobo, R. B., K. J. Ruschak, and B. A. Fitzgerald, "Gravure Coating Feed Apparatus," U.S. Patent No. 5,581,389 (1997).
Max Daetwyler Corporation, "MDC Doctor Blade Technical Manual," product literature of Max Daetwyler Corp., Huntersville, NY (1994).
Rabinowicz, E., *Friction and Wear of Material* (*2nd Edition*)," Wiley, New York (1995).
Rutherford, B., ed., *Gravure: Process and Technology*," Gravure Association of America, Rochester, NY (1991).
Walters, D. W., and R. B. Lobo, "Method for Engraving a Gravure Cylinder" U.S. Patent No. 5,426,588 (1995).

Manuscript received Feb. 15, 1999, and revision received Aug. 16, 1999.